



Politecnico
di Bari

Repository Istituzionale dei Prodotti della Ricerca del Politecnico di Bari

A stereo photogrammetry scanning methodology, for precise and accurate 3D digitization of small parts with sub-millimeter sized features

This is a pre-print of the following article

Original Citation:

A stereo photogrammetry scanning methodology, for precise and accurate 3D digitization of small parts with sub-millimeter sized features / Galantucci, L.M., Pesce, M., Lavecchia, F.. - In: CIRP ANNALS. - ISSN 0007-8506. - 64:1(2015), pp. 507-510. [10.1016/j.cirp.2015.04.016]

Availability:

This version is available at <http://hdl.handle.net/11589/1000> since: 2025-02-27

Published version

DOI:10.1016/j.cirp.2015.04.016

Publisher:

Terms of use:

(Article begins on next page)

Manuscript Number: 2015-P-17R3

Title: A stereo photogrammetry scanning methodology, for precise and accurate 3D digitization of small parts with sub-millimeter sized features

Article Type: Annals - Vol.1 - 2015

Keywords: 3D-Image processing, Reverse engineering, Photogrammetry

Corresponding Author: Prof. Luigi Maria Galantucci, Ph.D. MSE

Corresponding Author's Institution: Politecnico di Bari

First Author: Luigi Maria Galantucci, Ph.D. MSE

Order of Authors: Luigi Maria Galantucci, Ph.D. MSE; Marta Pesce, MSE Ind; Fulvio Lavecchia, Ph.D,MS, Ind Eng

Abstract: In this paper is presented a scanning methodology based on close-range stereo photogrammetry, suitable for precise and accurate 3D digitization of objects of few millimeters in length and features in sub- millimetre scale. The authors propose an efficient alternative to other scanning methodologies currently used for such applications, as the conoscopic holography, with the aim to reduce the scanning time and obtain a result which contains also information related to the real texture of the object. An experimental plan has been designed and implemented in order to investigate the accuracy and precision of the 3D scans.



A stereo photogrammetry scanning methodology, for precise and accurate 3D digitization of small parts with sub-millimeter sized features

Galantucci L.M.(1), Pesce M., Lavecchia F.

*Dipartimento di Meccanica, Matematica e Management, Politecnico di Bari
Viale Japigia 182, 70126 Bari, Italy*

This paper presents a scanning methodology based on close-range stereo photogrammetry, suitable for precise and accurate 3D digitization of objects of few millimeters in length and features in sub-millimeter scale. The authors propose an efficient alternative to other scanning methodologies currently used for such applications, as the conoscopic holography, with the aim to reduce the scanning time and obtain a result which also contains information related to the real texture of the object. An experimental plan has been designed and implemented in order to investigate the accuracy and precision of the 3D scans.

3D-Image processing, Reverse engineering, Photogrammetry

1. Introduction

The need of fast and cost effective instruments for 3D scanning and for measuring small manufactured parts is rapidly increasing, due to increasing relevance of micro components, fabricated with new methods and technologies [1–3]; using ultra-precise milling centers it is possible to obtain micrometer part accuracy [4]. For many products, as the micro injection molds or the micro EDM tools, not only the accuracy of linear or angular measurement is important, but often also to assess the quality and the precision of very complex three dimensional sub millimeter features. These metrological requirements can be achieved by adopting several methods [5]. In [6] is reported a survey of the current available technology for the measurement of complex 3D surfaces. The X-ray computer tomography is used to perform a non-destructive test for defects inspection [6] and for many micro and Nanometrology applications [7,8], such as scaffolds [9] and diesel nozzle orifices [10]. Coordinate measuring machines (CMM), with touch or optical probing, have been used for this purpose [11], but they evidence many limitations: touch probe can deform delicate parts in the contact points, and digitizing speed is too limited [12–14]; optical probing have limitations in measuring high surface slopes and they have a poor lateral resolution, due to the diffraction [14,15]. CMMs are expensive and large in size, and some economic and compact CMM systems have been developed only recently [16,17]. CMMs, conoscopic holography and X-ray tomography cannot return 3D models with the object natural texture.

In the past, photogrammetry was not considered able to scan and measure small parts and complex surfaces [6]. In recent works [18,19], on the contrary, new possibilities to use photogrammetry for accurate 3D scans of small object have been assessed, also for sub millimeter scale [20]. In [21] the influence of several factors is analyzed on the accuracy and precision obtained measuring small objects using close range digital photogrammetry.

In this work the authors propose a precise, rapid and cost effective photogrammetric scanning system with a rotary table suitable to scan small parts with complex surfaces and sub-millimeter features. This approach allows to scan small free form objects having a high aspect ratio, with high deep of field,

compared to other optical methods. Major limitations highlighted for this instrument are the need to scale the digital model through an additional measuring instrument and the need to study the calibration process to eliminate any distortions in the model.

2. The scanning methodology

The photogrammetric scanning methodology has been developed in order to automate and improve the traditional technique for photogrammetric acquisition and reconstruction. Figure 1 shows a design of the prototype of the Photogrammetric Scanning System with Rotary Table (PSSRT), realized for the implementation of the experiment.

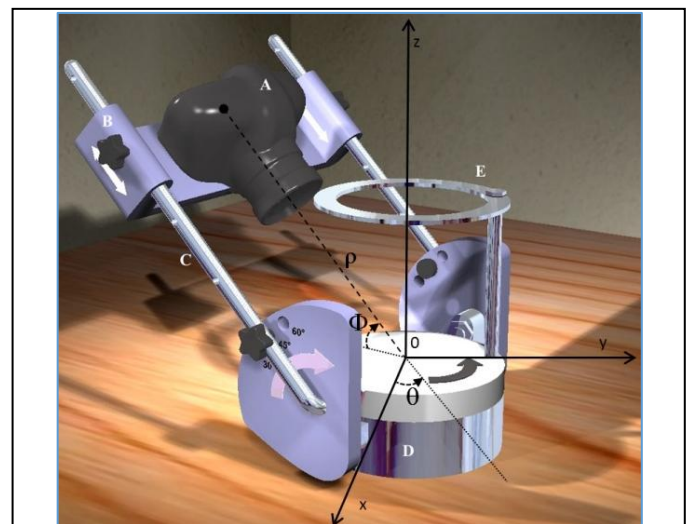


Figure 1: Design of the prototype realized for the implementation of the presented methodology: A) Digital SLR Camera; B) Platform for focus distance tuning; C) Rigid tubular frame for tilt angle tuning; D) Rotary Table; E) Light.

In the PSSRT the object is placed on a rotary table (D) which rotates at fixed steps (θ), while a Digital SLR Camera (A) is fixed on a platform (B), whose position can be adjusted along a rigid frame (C). The rigid frame (C) is designed to constrain the camera in a spherical path with radius (ρ) equal to the focal length; it

allows to regulate the tilt angle (Φ) of the camera. A LED lightening system (E) integrated with the rotor of the rotary table, ensures uniform and homogeneous lighting condition during the rotation.

In this system the choice of the lens is related to the maximum footprint dimension of the part, or of the rotating table. Only fixed focal length lens are used, having so fixed the focusing at known distances (ρ), which is adjusted regulating the position of the camera respect to the object through the sliding platform (B).

The tilt angle (Φ) can be regulated in function of the slope of the surfaces of the scanned object, increasing this angle if there is a prevalence of horizontal surfaces (flat component), or decreasing it if there is a prevalence of vertical surfaces (pillar component).

Once the position of the camera and the tilt angle have been fixed, the scan is performed shooting photos during a complete rotation of the table (360°). The rotation step angle between each shot (θ) is another important process parameter: reducing this step angle, a larger number of shots will be taken for a complete rotation, with a major percentage of overlapping among the photos (that could enhance the form features visibility and quality of the photogrammetric reconstruction), increasing the time for scanning and time for the computer photogrammetric processing of photos.

The method to overcome the major limitation, related to the absence of an internal scale of the 3D model obtained using photogrammetry, is to provide to the algorithm the spatial coordinates of the center of the sensor of the camera for each shot (external calibration).

The acquisition phase is fully automated and controlled remotely from a computer: the turntable rotates at a step angle, then stops, a shutter trigger is sent to the camera, and the image is acquired. This process is repeated until the turntable has completed a whole 360° turn. Then, the acquired images are elaborated using an image-based 3D modelling software [22].

3. Materials and methods

3.1 Part design

In order to supply a benchmark with complex surface and sub millimeter features, a test object in aluminum alloy, has been machined on a 3-axes machining center. The sample has a pyramidal geometry with square base (Figure 2) inspired by those used to calibrate stereo SEM (Scanning Electron Microscopes) images for photogrammetric applications [23].

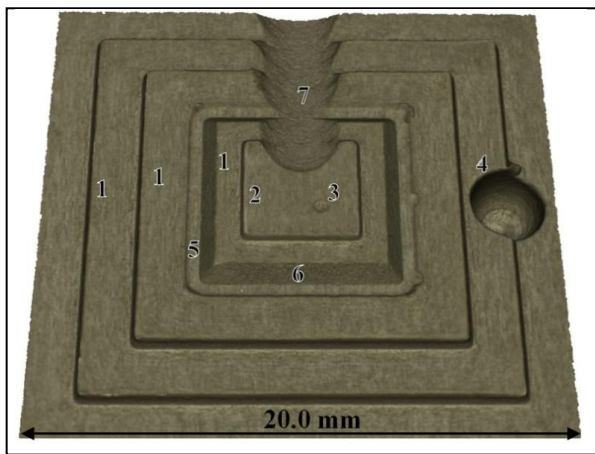


Figure 2: Image of the object used as benchmark and dimension of the basis.

It presents the following features and nominal dimensions:

- 1.three steps of 0.5 mm height;
- 2.one step of 0.2 mm height;

- 3.one blind hole $\varnothing 0.7$ mm and 0.08 mm depth;
- 4.one blind hole $\varnothing 3.0$ mm and 2.0 mm depth, done with a ball end mill;
- 5.one slot of 0.5 mm width and 0.1 mm depth;
- 6.one chamfer of 45° ;
7. one free form feature obtained with a spherical $\varnothing 3.0$ mm tool.

The sample results particularly suitable for the purpose of this study because it presents many regular form features and a free-form surface, and it allows to appreciate the capability of the proposed methodology.

3.2 Camera calibration

Digital photogrammetric algorithms need two types of calibration: external and internal. The external calibration is the procedure that gives the spatial position of the camera sensors, while the internal allows the radial and the decentering distortions of the lens to compensate [24]. Both calibrations can be automatically estimated by many software or obtained with specific calibration procedures. This work investigated the possibility to obtain a digital 3D model in 1:1 scale providing to the photogrammetric algorithms an external calibration, which can eliminate the need of an external metric reference scale.

Using the PSSRT, the external calibration can be provided giving the scanning process parameters directly ρ , Φ and θ . In this work, to eliminate possible manufacturing and assembly inaccuracies, the external calibration was performed in a preliminary phase through the acquisition of a planar calibration pattern of 50×30 mm, with 12 bit coded targets, positioned in the center of the rotary table (Figure 3). The targets have a little white circle in the middle, which enable to measure the coordinate of the center of each target. For this purpose the optical CMM DeMeet 400 has been used (accuracy in X = $5.33\mu\text{m}$, Y = $5.33\mu\text{m}$, Z = $4.33\mu\text{m}$).

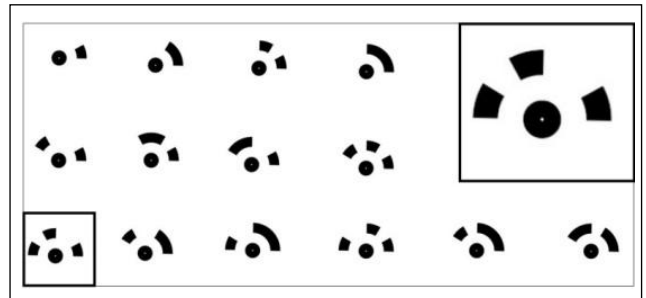


Figure 3: Pattern of 12 bit coded target used for the external camera calibration.

The acquired calibrator images are elaborated through an image-based 3D modelling software [22]. This software is based on the Structure-From-Motion (SFM) and Dense Multi-View 3D Reconstruction (DMVR) algorithms, and allows to build 3D models by unordered image collections that depict a scene, or an object, from different viewpoints [25]. In the first step the software performs the alignment of the images, on the basis of common points in the source photos, and matches them with a SIFT (Scale-invariant feature transform) like approach [26].

At this step, giving the previously measured coordinates of the coded target, automatically marked by the software, the real position of the camera in the 3D space is computed for each shot.

This set of camera positions (external calibration) is required for the next step, which is the dense points cloud building, using the pair-wise depth map computation algorithm, constructed on the basis of the measured or estimated camera positions and pictures themselves. Using the described scanning methodology with the PSSRT realized, it is possible to affirm that the positions of the camera in the space are constant and time-invariant, and

therefore they can be used for the construction of the 3D digital model of the object to be scanned.

3.3 Experimental design

In order to investigate the influence of the key factors on the scanning methodology capability, an experimental design has been realized. For this purpose, a three-level full factorial design was carried out. According to the literature, the following three factors were selected: external calibration (X_1), amplitude of the turntable rotation step angle (X_2), which determines the overlap of the images, and tilt angle of the camera (X_3) (Table 1). The high and low values for each factor were defined considering the limits of the available experimental setup according with literature, photogrammetric rules acquisition and previous experiences.

For each scanning condition of the experimental plan, three acquisitions were collected and executed in a random order. For the experimental realization a digital SLR camera Canon 40D (Effective pixels 10 megapixels, Sensor size APS-C 22.2 x 14.8 mm) with Canon EF 50 mm 1:1.8 II lens focused to infinity and a Kenko Extension Tubes of 36 mm length were used.

4. Results and discussion

4.1 Accuracy statement

The accuracy statement was performed by executing a 3D comparison of all models with a digital model obtained with Optimet Conoscan 4000 (with “Conoprobe Mark 3.0 HD” sensor and 50 mm lens that allow to perform 3D measurement with 2 mm working range, measurement errors of 2.5 μm and repeatability 3σ of 0.5 μm). The result of all 3D comparison, expressed as average distance between the test and the reference surface as well as the standard deviation of the distances for each comparison, is reported in Figure 4. It is possible to observe that the average distances and the related standard deviations are very limited in all cases, except for run 5, run 10 and run 18, the three executed with the investigated factors at the same level ($X_1 = H$, $X_2 = H$ and $X_3 = L$). Color maps allow to graphically visualize the distances between the test and the reference surfaces. In Figure 5 the best and the worst results of the 3D comparisons (without considering runs 5, 10 and 18) are reported.

4.2 Characterization of the 3D models

To quantitatively characterize the 3D digital models of the test object, four response variable were taken into account: three linear measurement (H_1 , H_2 and H_3 in Figure 6) and one cubic measurement (V – volume inside the model surface). Each linear measurement was measured three times. The standard deviation of each measurement is between 0.0 and 0.003 mm. Measuring by Optimet Conoscan 4000, H_1 is equal to 1.740 mm, H_2 is equal to 0.217 mm, H_3 is 0.081 mm and the volume inside the model surface is 238.19 mm^3 . The volume was measured in the 3D model using a plane fixed at a given level of Z , close to the base of the pyramid. Since all models are aligned in the same reference system, the measurement of the volume is a comparable parameter, and it is useful to ascertain the quality of the results; this measure could synthetize the three dimensionality of the model. The difference of the response variables H_1 , H_2 , H_3 and V measured on the test and the reference models, are reported in Table 2.

Table 1 Factors of the implemented three-level full factorial design

Factor	L - Low value	H - High value
X_1 - External calibration	No	Yes
X_2 [deg] - step angle	5	20
X_3 [deg] - tilt angle	30	60

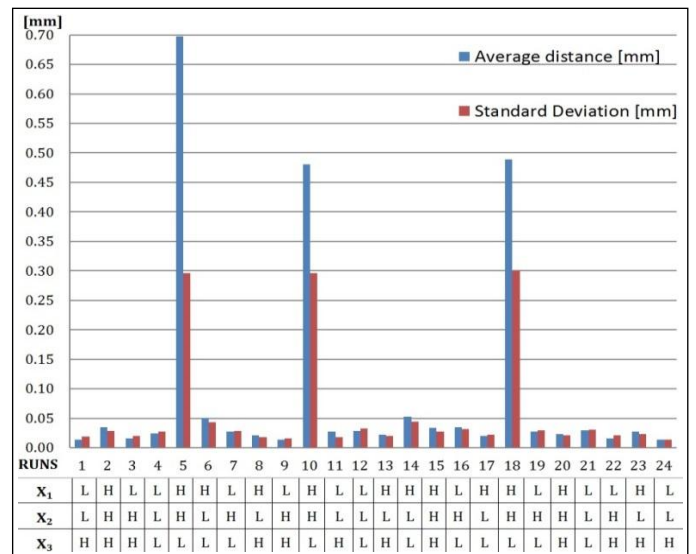


Figure 4: Average distances and standard deviations of the distances measured between the test and the reference model in the 3D comparisons.

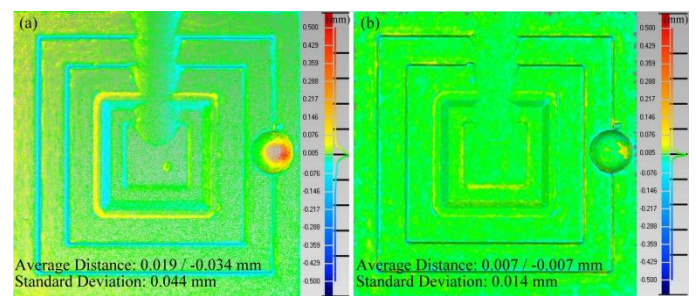


Figure 5: The color maps obtained for the 3D comparison of (a) Run 14 and (b) Run 24.

Table 2: Difference between H_1 , H_2 , H_3 and volume measured using Optimet and PSSRT

Δ between Optimet and PSSRT	A $X_1=L$ $X_3=L$	B $X_1=H$ $X_3=L$	C $X_1=L$ $X_3=H$	D $X_1=H$ $X_3=H$
ΔH_1 [mm]	0.007	0.146	0.005	0.012
ΔH_2 [mm]	0.003	0.019	0.002	0.002
ΔH_3 [mm]	0.004	0.010	0.003	0.002
ΔV [mm^3]	0.360	77.762	0.603	0.845

4.3 Influence of the factors

The 3D comparisons show the tilt angle (X_3 factor) strongly influenced the final result. When $X_3 = H$, the 3D digital models are precise and have the correct 1:1 scale. The precision of the PSSRT calculated as the standard deviation of the three linear response variables H_1 , H_2 and H_3 measured under controlled conditions ($X_1 = H$ and $X_2 = H$), is 0.003mm, 0.002 mm and 0.001 mm respectively, while the trueness is 0.012 mm, 0.004 mm, and 0.003 mm respectively.

The step angle X_2 has a negligible effect on the result, because an amplitude of rotation of 20° allows for the considered geometry a good visibility of the form features and good

overlapping of the frames. The choice of a step angle of 5° ($X_2 = L$) quadruplicate the number of frames, for as this benchmark does not improve the result, and gives only a negative impact, because the acquisition time increases proportionally to the number of pictures and the processing time increases more than proportionally. This observation suggests that lower step angles could be adopted only if a better visibility of some small and complex form features can be obtained.

When the tilt angle (X_3) is set to Low level (L), the 3D comparisons show that the digital models have a wrong scale factor. The result becomes even worst when X_2 change from Low (L) to High (H) level, reducing the images overlap.

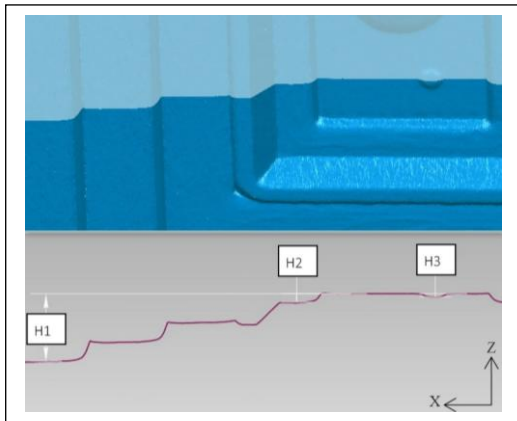


Figure 6: Linear measurements considered as response variables.

As 3D comparisons showed that X_2 is the factor which less affects the 3D models building process, the results reported in the Table 2 have been grouped into four sets (A, B, C and D), to assess the effect of X_1 and X_3 factors, which seem to have greater influence on the result. Thus each value in Table 2 is the arithmetic mean of six values.

The results highlight that the greatest differences are reported in column B ($X_1 = H, X_3 = L$); the comparison of these values with the values reported in column A ($X_1 = L, X_3 = L$) allows to affirm that the differences are due to the X_1 factor, that means the external calibration performed at 30° tilt angle, introduces a significant scale error in the 3D model.

When X_3 factor is set to High level (H), the external calibration performed at 60° tilt angle introduces measurement differences comparable with those of non-calibrated models (see Table 2 – columns C and D), having the great advantage that the models are automatically scaled.

5. Conclusions

In this work, an innovative and rapid methodology suitable to perform 3D measurement on parts with relatively large footprint dimensions and free form sub-millimeter sized features, has been presented. Using an external calibration, the implemented methodology is able to overcome one of the major limitations of the scanning photogrammetric approach, the absence of an internal scale of the 3D model, allowing to obtain a digital 3D model in 1:1 scale without the need of an external metric reference scale.

An appropriate experimental plan enabled the investigation about the parameters that greatly influence the final result. Respect to the considered benchmark geometry, the tilt angle (X_3) has proved to be the most influent factor: when it is set to 60° (H), the external calibration is performed properly and the 3D models are precise and accurate (precision 0.001 – 0.003 mm, trueness 0.001 – 0.012 mm), while for very low values, such as 30° , the

adopted external calibration process fails, and the final result shows significant scale errors.

Acknowledgement

This research is funded by the Italian Ministry of Education, University and Research, PON02_00576_3333604 "INNOVHEAD"

References

- [1] Malek CK, Saile V (2004) Applications of LIGA technology to precision manufacturing of high-aspect-ratio micro-components and -systems: a review. *Microelectronics J* 35(2):131–143.
- [2] Qin Y, Brockett A, Ma Y, Razali A, Zhao J, Harrison C, et al. (2009) Micro-manufacturing: research, technology outcomes and development issues. *Int J Adv Manuf Technol* 47(9-12):821–837.
- [3] Bauer W, Knitter R, Emde A, Bartelt G, Göhring D, Hansjosten E (2002) Replication techniques for ceramic micro-components with high aspect ratios. *Microsyst Technol* 9(1-2):81–86.
- [4] Byrne G, Dornfeld D, Denkena B (2003) Advancing cutting technology. *CIRP Ann - Manuf Technol* 52(2):483–507.
- [5] Hansen HN, Carneiro K, Haitjema H, De Chiffre L (2006) Dimensional Micro and Nano Metrology. *CIRP Ann - Manuf Technol* 55(2):721–743.
- [6] Savio E, De Chiffre L, Schmitt R (2007) Metrology of freeform shaped parts. *CIRP Ann - Manuf Technol* 56(2):810–835.
- [7] Dierick M, Van Hoorebeke L, Jacobs P, Masschaele B, Vlassenbroeck J, Cnudde V, et al. (2008) The use of 2D pixel detectors in micro- and nano-CT applications. *Nucl Instruments Methods Phys Res Sect A Accel Spectrometers, Detect Assoc Equip* 591(1):255–259.
- [8] Fisher RF, Hintenlang DE (2008) Micro-CT Imaging of MEMS Components. *J Nondestruct Eval* 27(4):115–125.
- [9] Ho ST, Huttmacher DW (2006) A comparison of micro CT with other techniques used in the characterization of scaffolds. *Biomaterials* 27(8):1362–1376.
- [10] Wu Z, Li Z, Huang W, Gong H, Gao Y, Deng J, et al. (2012) Comparisons of nozzle orifice processing methods using synchrotron X-ray micro-tomography. *J Zhejiang Univ Sci A* 13(3):182–188.
- [11] Yang P, Takamura T, Takahashi S, Takamasu K, Sato O, Osawa S, et al. (2011) Development of high-precision micro-coordinate measuring machine: Multi-probe measurement system for measuring yaw and straightness motion error of XY linear stage. *Precis Eng* 35(3):424–430.
- [12] Meli F, Küng A (2007) AFM investigation on surface damage caused by mechanical probing with small ruby spheres. *Meas Sci Technol* 18(2):496–502.
- [13] Vliet WP Van, Schellekens PH (1996) Accuracy limitations of fast mechanical probing. *CIRP Ann - Manuf Technol* 45(1):483–487.
- [14] Hoffmann J, Weckenmann A, Sun Z (2008) Electrical probing for dimensional micro metrology. *CIRP J Manuf Sci Technol* 1(1):59–62.
- [15] Schwenke H, Neuschaefer-Rube U, Pfeifer T, Kunzmann H (2002) Optical methods for dimensional metrology in production engineering. *CIRP Ann - Manuf Technol* 51(2):685–699.
- [16] Goo C-S, Jun MBG, Saito A (2012) Probing system for measurement of micro-scale components. *J Manuf Process* 14(2):174–80.
- [17] Fan KC, Fei YT, Yu XF, Chen YJ, Wang WL, Chen F, et al (2006) Development of a low-cost micro-CMM for 3D micro/nano measurements. *Meas Sci Technol* 17(3):524–532.
- [18] Nguyen C, Lovell D, Oberprieler R, Jennings D, Adcock M, Gates-Stuart E, et al (2013) Virtual 3D Models of Insects for Accelerated Quarantine Control. *2013 IEEE Int. Conf. Comput. Vis. Work., IEEE* 161–167.
- [19] Nguyen C V, Lovell DR, Adcock M, La Salle J (2014) Capturing natural-colour 3D models of insects for species discovery and diagnostics. *PLoS One* 9(4):e94346.
- [20] Galantucci LM, Lavecchia F, Percoco G (2013) Multistack Close Range Photogrammetry for Low Cost Submillimeter Metrology. *J Comput Inf Sci Eng* 13(4):044501.
- [21] Galantucci LM, Percoco G, Ferrandes R (2006) Accuracy issues of digital photogrammetry for 3D digitization of industrial products. *Rev Int D'ingénierie Numérique* 2(1-2):29–40.
- [22] Agisoft. Photostan Professional Edition. <http://www.agisoft.com/features/professioniprof-edition/>. (accessed January 15, 2015)
- [23] Sinram O, Ritter M, Kleindick S, Schertel A, Hohenberg H, Albertz J (1976) Calibration of an SEM, using a nano positioning tilting table and a microscopic calibration pyramid. *Int Arch Photogramm Remote Sens Spat Inf Sci* 34(5):210–215.
- [24] Brown D-C (1971) Close-Range Camera Calibration, *Photogrammetric Engineering* pp. 855–866.
- [25] Koutsoudis A, Vidmar B, Ioannakis G, Arnaoutoglou F, Pavlidis G, Chamzas C (2014) Multi-image 3D reconstruction data evaluation. *Journal of Cultural Heritage* 15(1):73–79.
- [26] Lowe D-G (2004) Distinctive image features from scale-invariant keypoints. *International journal of computer vision* 60(2): 91–110.